Agricultural and Forest Meteorology 287 (2020) 107926

Contents lists available at ScienceDirect

Agricultural and Forest Meteorology

journal homepage: www.elsevier.com/locate/agrformet

# Quantification of uncertainties introduced by data-processing procedures of sap flow measurements using the cut-tree method on a large mature tree

Morgane Merlin[a,*], Kevin A. Solarik[a,b], Simon M. Landhäusser[a]

[a] Department of Renewable Resources, University of Alberta, 4-42 Earth Sciences Building, Edmonton, AB T6G 2E3, Canada
[b] National Council for Air and Stream Improvement, Inc., 2000 McGill College Avenue, 6th Floor, Montréal, QC H3A 3H3, Canada

ARTICLE INFO

*Keywords:*
Heat ratio method (HRM)
Sap flow
Cut-tree method
Zero-flow
Sapwood area
Uncertainty

ABSTRACT

Sap flow sensors are crucial instruments to understand whole-tree water use. The lack of direct calibration of the available methods on large trees and the application of several data-processing procedures may jeopardize our understanding of water uptake dynamics by increasing the uncertainties around sensor-based estimates. We directly compared the heat ratio method (HRM) sap flow measurements to water uptake measured gravimetrically using the cut-tree method on a large mature aspen tree to quantify those uncertainties for ten consecutive days. The influence of the azimuthal position of the sensors and the application of different data-processing procedures on the accuracy of the sap flow sensors' estimates was assessed using different metrics. Overall, the sap flow measurements showed high temporal precision with the gravimetric data. Azimuthal and radial variability of measured sap flux density showed the most substantial effect on the accuracy of the sensors' estimates of whole tree sap flow. The zero-flow corrections applied altered the accuracy and linearity of the sensors' measurements at the hourly scale, while the sapwood area method used had a lesser impact. Across the ensemble of available data-processing procedures, the cumulative whole-tree water uptake estimates for five consecutive days from the sensor diverged from the gravimetric measurements by less than 1% to more than 50% depending on the sensors azimuthal position and data corrections applied. This study illustrates some of the uncertainties associated with the methodological approaches chosen when using sap flow sensors to estimate water uptake in tall and large diameter trees.

## 1. Introduction

Heat-based sap flow methods have become a principal means to non-destructively provide whole-tree water use estimates across spatiotemporal scales (Hassler et al., 2018), while also improving our understanding of the impact(s) of a changing climate (Berdanier and Clark, 2018; Zhang et al., 2016) and forest management practices (Doody et al., 2015) on forested landscapes. Several sap flow methods are available to measure tree-water use (Fernández et al., 2017) using heat as a tracer for sap flow. Calculating whole-tree sap flux rates using heat tracers requires several steps of data-processing (Looker et al., 2016; Peters et al., 2018). Proper estimation of the sapwood thermal diffusivity as well as corrections for probe misalignment and wounding need to be considered (Burgess et al., 2001; Burgess and Downey, 2018;

*Abbreviations: AD*, average of the two thermistor depths from the SFM1 HRM probes, the Outer and Inner thermistors; *MD*, thermistor depth with the maximum magnitude - *i.e.* largest range of sap flux density measurements from the SFM1 HRM probes, between the Outer and Inner thermistors; *SS*, study-specific zero-flow correction; *PD*, Pre-dawn zero-flow correction; $PD_d$, Daily pre-dawn zero-flow correction; *LR*, Linear regression zero-flow correction; *DLR*, Double linear regression zero-flow correction; $SA_{true}$ ($cm^2$), true sapwood area measured on tree disks; $SA_{tc}$ ($cm^2$), sapwood area derived from a unique sapwood length for each of the cardinal directions; $SA_{tc\text{-}avg}$ ($cm^2$), sapwood area derived from the average of the sapwood lengths from the four cardinal directions; $SA_{tc\text{-}opp}$ ($cm^2$), sapwood area derived from the average of the sapwood lengths from two opposite cardinal directions; $SA_{tc\text{-}per}$ ($cm^2$), sapwood area derived from the average of the sapwood lengths from two perpendicular cardinal directions; *R*, radial profile of sap flux density; $J_s$ ($g\,cm^{-2}hr^{-1}$), sap flux density at each cardinal orientation *i*; $Q_i$ *or* $Q$ ($L\,hr^{-1}$), whole-tree hourly sap flux rate calculated from the sensor placed at each cardinal orientation *i*; $Q_{quarter}$ ($L\,hr^{-1}$), whole-tree hourly sap flux rate calculated as the sum of the four cardinal sap flux rates; $Q_{scale}$ ($L\,hr^{-1}$), gravimetrically-measured whole-tree hourly sap flux rate; $Q^d$ ($L\,d^{-1}$), whole-tree daily sap flux rate calculated from the sensor placed at each cardinal orientation; $Q^d_{scale}$ ($L\,d^{-1}$), gravimetrically-measured whole-tree daily sap flux rate; $Q^c$ (L), whole-tree cumulative water uptake calculated from the sensor placed at each cardinal orientation; $Q^c_{scale}$ (L), gravimetrically-measured whole-tree cumulative water uptake; *VPD* (kPa), Atmospheric vapor pressure deficit

* Corresponding author.
*E-mail address:* morgane@ualberta.ca (M. Merlin).

https://doi.org/10.1016/j.agrformet.2020.107926
Received 9 October 2019; Received in revised form 21 January 2020; Accepted 30 January 2020

Marshall, 1958). Zero-flow determination is an additional crucial step, for which a range of empirical, systematic (Granier, 1987; Lu et al., 2004), and physically-based (Burgess and Downey, 2018; Oishi et al., 2008) methods are available. Additionally, strong radial and circumferential variations (Van de Wal et al., 2015) are often ignored, potentially leading to over- or under-estimating whole-tree water use when extrapolating a single sensor measurement across the entire stem. A global assessment of the impact of the combination of those data-processing steps on sap flow studies is currently lacking (but see Looker et al., 2016; Peters et al., 2018; Rabbel et al., 2016; Van de Wal et al., 2015 among others, addressing individual data-processing approaches), challenging the interpretation, comparison, and integration of individual tree-based studies when used in large-scale ecohydrology models.

A general quantification of the uncertainties generated by both the sap flow sensor method itself and the combination of methodological decisions and data-processing procedures on large mature trees is lacking, but crucial (Flo et al., 2019), particularly when attempting to derive landscape-scale processes (*e.g.* ecosystem water and carbon fluxes, catchment hydrological and vegetation responses to climate and land-use changes; Bonan, 2008; Schlesinger and Jasechko, 2014). Calibration studies addressing the accuracy of the sap flow measurements in woody plants have been previously conducted (see the Supplementary Material in Flo et al. (2019) for a list of studies and calibration materials), however, many of them were mostly focused on smaller trees (less than 10 cm in diameter), shrubs, or branch segments, which are unlikely to provide reliable or appropriate estimates of water-use in larger diameter trees. To date, only a few studies have directly assessed the accuracy of sap flow sensors in estimating the water uptake of large mature trees (Olbrich, 1991; Roberts, 1977; Vertessy et al., 1997). However, the height (>10 m), diameter (>20 cm) and weight of mature forest trees presents experimental and logistical challenges for obtaining a direct measurement of water uptake to compare with the sap flow sensors' estimates, and thus, these studies are very limited in scope. The anatomical, morphological, and physiological variability in the stem of large mature trees can result in potentially strong diverging patterns between and within-trees in sap flux densities (Cohen et al., 2008; Shinohara et al., 2013; Van de Wal et al., 2015). The choice of the method in correcting for zero-flows and extrapolating to whole-tree sap flux rates may increase the error in sensor-based estimates of water use of an individual tree. Ultimately, this can jeopardize the interpretation of climate-response analyses and stand-level water uptake estimates for large and mature trees across temporal and spatial scales.

In this study, we aimed to: (1) quantify the extent of uncertainty in sap flow measurements related to circumferential variability, the application of different sapwood area estimation methods and zero-flow corrections; and (2) assess the impact of each and the combination of these factors on the relationship with climate variables and estimates of cumulative whole-tree water uptake. We used heat ratio method (HRM) sap flow heat-pulse sensors (Burgess et al., 2001) which have shown relatively good performance in accuracy when compared to other sap flow methods (Flo et al., 2019). Furthermore, we used the cut-tree technique to directly measure trunk water uptake gravimetrically by immersing the stem of a large tree (20 m tall, 35 cm in diameter) in water (Roberts, 1977). Using this technique, we can directly compare the HRM sap flux estimates to the gravimetrically-measured water uptake, and then quantitatively assess the uncertainty and error associated with several data-processing methods applied to the sap flow data.

## 2. Materials and methods

### 2.1. Study site and climate data

The study was carried out in Thorhild County (54°17′11.6″ N, 112°46′08.6″ W), approximately 120 km northeast of Edmonton, Alberta, Canada. The site is located within the dry mixedwood natural sub-region of the boreal region, composed of a mixture of trembling aspen (*Populus tremuloides* Michx.) and white spruce (*Picea glauca* (Moench) Voss), surrounded by agricultural lands. The selected trees for the study were part of a 60 - 70-year-old trembling aspen dominated stand (~ 600 stems per hectare). The stand is located on a relatively flat site with a well-drained orthic gray luvisol that is easily accessible by machinery to access the trees' crown. This region has a mean temperature of −13.4°C in January and +16.6 °C in July and annual precipitation of 478.7 mm (1981–2010 climate normal, Athabasca station, 54°82'00" N, 113°54'00" W)(Alberta Climate Information Service (ACIS), 2018). Hourly climatic data (relative humidity (%), air temperature ( °C)) was retrieved from the Alberta Climate Information Service (Alberta Climate Information Service (ACIS), 2018) for the Abee weather station (54°14′16″N 113°01′40″W), located 16.6 km from the research site. For all sources of climatic data, vapor pressure deficit (VPD, kPa) was calculated. The whole study was carried out between July 15th, 2017 and August 28th, 2017.

### 2.2. Sap flow measurements

A mature (60-year-old) healthy trembling aspen (deciduous broad-leaved species with diffuse-porous wood) was selected as the focus tree for this study, on a slightly elevated area of the study site. The focus tree was a 20 m tall co-dominant tree in the stand, had a diameter of 28.8 cm at breast height (1.3 m) and a relatively symmetrical crown (~ 6–7 m in diameter, starting at 11 m above the ground). The focus tree had no apparent deformities in the stem or indications of fungal infection or decay (which was confirmed later after cutting). In addition to the focus tree, three co-dominant trembling aspen trees were also selected as controls for the entire period of the experiment. These trees were within the vicinity (10–15 m) of the focus tree and had similar tree and site characteristics. More information on the tree characteristics and sensor locations are provided in Supplementary Material Table A.1.

The focus tree was equipped with four HRM sap flow sensors installed at the four cardinal directions (north, east, south, and west) at a trunk height of 2.5 m. The sensors were not installed at the commonly used 1.3 m trunk height as the cutting procedure removed the lowest 2 m of trunk of the focus tree (see Supplementary Material Fig. A.2). The three control trees were each equipped with one HRM sap flow sensor located at 1.3 m on the north-facing aspect. The difference in height between the sensors on the focus and control trees was assumed negligible for the purpose of the study. Sensors were installed on July 17th and 18th, 2017, and recorded sap flux density at 10 min intervals between July 18th and August 22nd, 2017.

The HRM sap flow technique was chosen due to its ability to detect and quantify low flows more reliably than other techniques (Burgess et al., 2001). We used commercially available HRM sap flow sensors (SFM1, ICT International Pty Ltd., Armidale, Australia). The sensors consist of a three individual needles (length: 35 mm; diameter: 1.3 mm): a heater needle delivering a 20 J heat pulse for 2.5 s every 10 min, a downstream and upstream needles with two thermocouples - thermistors - spaced 17.5 mm apart and positioned 12.5 (Inner thermistor) and 27.5 (Outer thermistor) mm from the needle base. The needles are each installed 0.5 cm apart. Power to all sap flow sensors was supplied by external 12 V deep cycle marine batteries, and their charge was maintained with solar panels. Application, set-up, and limitations of the SFM1 HRM sap flow sensors have been described previously (Bleby et al., 2004; Burgess and Downey, 2018; Forster, 2017).

### 2.3. Cut-tree procedure

The study set-up and cutting procedure are shown in Supplementary Material Figs. A.1 and A.2, described hereafter. Prior to cutting the focus tree, a wooden structure was built to support the tree. The wooden structure had two platforms (4.5 m × 4.5 m) with enforced beams placed at 4.5 m and 9.0 m height above ground, and an additional enforced support beam at 2.0 m above ground. Additional support of the tower was provided by securing it to neighbouring (non-study) trees and using soil anchors. To secure the suspended position of the cut tree and to allow it to rest on the enforced support beams, friction blocks were used. These friction blocks were made of 5 × 10 × 20 cm blocks of hardwood wood (oak), where each block contained 20–30 wood screws (7.6 cm long) inserted with their tips protruding 2–5 mm from the block. Several of these blocks were arranged around the circumference of the trunk, each resting on the three respective support beams once tightly strapped to the stem using ratchet straps. Once cut, the ring of friction blocks ensured that the tree remained suspended and supported by the cross beams. The screw tips did not affect the xylem tissue and impacted only the bark and potentially some of the outer portions of the phloem.

Since the HRM sap flow sensors estimates of water uptake of the focus tree were to be compared directly with a the cut-tree method (Roberts, 1977), the focus tree needed to be cut at its base and inserted into a bucket of water. To avoid cavitation of the sapwood during cutting, the focus tree needed to be pre-cut underwater. A flexible temporary watertight container was used to allow for a pre-cut underwater. This temporary container was made from heavy-duty rubber material (pond liner) that was wrapped, secured, and sealed around the trunk (height of 1.0 m). The outer rim of the temporary container was then attached to the support structure. An initial girdling cut was made underwater and inside the water-filled temporary container using a chainsaw. This cut was around the circumference of the stem and about 15 cm deep to ensure all sapwood was included in this cut. The center part of the heartwood was left intact to support the tree initially. After the initial girdling cut, two additional cuts were performed cross-sectionally; one full cut directly below the temporary container and a second full cut at ground level; fully removing the portion of the trunk located underneath the temporary container. Now supported by the wooden structure, a large poly-ethylene bucket (600 L) sitting on a large commercial scale 1000 kg capacity floor scale (FSP 3 × 3′ - Anyload, Fairfield, NJ, USA) was placed under the cut trunk. To monitor and record water uptake as a negative weight changes (200 g precision), a weight indicator connected to a storage unit (480Plus weight indicator and Go-Between Data Storage unit, Rice Lake Weighing Systems, Rice Lake, WI, USA) was used. Weights were recorded every sixty seconds. After the scale and bucket were placed under the tree, the bucket was filled with water. A final full cut of the trunk was made underwater, approximately 10 cm above where the initial girdling cut was made, providing a clean-cut surface and the ability to remove the temporary container (*i.e.* pond liner). The newly-exposed cut end of the tree was now submerged (~30 cm) under water in the large bucket. Throughout the entire study period, the cut end of the tree was continuously submerged to avoid cavitation. To reduce the blockage of xylem vessels (through wounding, accumulation of phloem exudates, or from impurities in the water), a sharp broad-bladed planer was used daily (at dawn) for the entirety of the study to shave the xylem on the cut end. Water levels within the bucket were checked daily and were topped up when needed. Additionally, a fresh chainsaw cut of the exposed end was made 5 and 10 days following the initial cut; to minimize surface blockage of xylem vessels in the sapwood. Evaporation from the container was prevented by covering the top of the bucket with a black plastic sheet sealing it around the trunk of the tree. Inputs from precipitation were excluded by covering the lowest platform and sides of the structure with tarps that shielded the bucket from all precipitation.

Transpiration rates were measured in the crowns using the LI-6400XT portable photosynthesis system (LiCor, Inc., Lincoln, NE, USA) on three shade leaves (lower branches in the canopy) and three sun leaves (top branches of the canopy) accessed using an articulated boom lift. Measurements were taken 4 and 8 days after the cut-tree was submerged in the bucket between 10:00 and 14:00 on the focus tree and a control tree during which the cuvette settings were 400 ppm $CO_2$; 60% incoming relative humidity; and ambient leaf temperature and light levels. Leaf water potential was measured on three upper canopy leaves using a Scholander pressure bomb (Scholander et al., 1965) (model 600, PMS Instrument Company, Albany, OR, USA) to assess the water status of the crown. One measurement was made at noon eight days after the cut, and another measurement 14 days after the cut, before dawn (06:00–07:00) .

### 2.4. Sap flow data baseline corrections

The raw heat velocities from the sap flow sensors were initially corrected for the wounding coefficient (Burgess et al., 2001; Marshall, 1958) using the software Sap Flow Tool (v1.4.1. ICT International Pty Ltd., Armidale, NSW, Australia). Wound diameter was visually quantified for all sensor locations from the sapwood cross-section (focus tree) or tree cores (control trees) and ranged between 0.25 and 0.30 cm. The estimation of the sapwood thermal diffusivity is required in the calculations of sap flux density. The thermal diffusivity of fresh sapwood was calculated for each sensor location on the focus tree. Fresh sapwood samples from each sensor location were taken directly after the removal of the sap flow sensors at the end of the experiment to determine fresh weight, volume (using Archimedes' principle) and oven-dried weight (72 h at 70 °C). Specific heat of the dry wood matrix and sap were assumed constant, and equal to 1.2 $10^3$ J $kg^{-1}$ $°C^{-1}$ and 4.19 $10^3$ J $kg^{-1}$ $°C^{-1}$ respectively. We obtained thermal diffusivity values ranging from 2.25 $10^{-3}$ to 2.29 $10^{-3}$ $cm^2$ $s^{-1}$. We used the average thermal diffusivity measured at 1.3 m high on the focus tree at the four cardinal directions for application to the sap flow sensor's data of the control trees. Before further processing, the 10-minutes sap flux densities were averaged into 30 min intervals to reduce variance.

### 2.5. Radial integration, zero-flow determination and sapwood area calculations

Three data-processing steps are necessary to convert sap flux density measurements to whole-tree sap flux rates. We evaluated the different options available based on published methods and most commonly applied approaches for the radial integration (Burgess and Downey, 2018; Link et al., 2014), the zero-flow determination approaches (Burgess and Downey, 2018; Granier, 1987; Lu et al., 2004; Oishi et al., 2016, 2008), and the sapwood area calculations (Looker et al., 2016). These three variables were evaluated to assess their relative contribution to the accuracy of the estimates of whole tree sap flow obtained with the HRM sap flow sensors compared to gravimetrically-measured water uptake at the hourly timescale and in terms of cumulative water uptake.

**Radial integration**: the HRM sensor is equipped with two thermistors (an inner, the shallowest measuring point, and outer) to measure the sap flux density along a fixed depth of sapwood. Before correcting for zero-flow and extrapolating to the entire sapwood area, two measures can be used that are derived from the two thermistors:

- *Maximum magnitude depth (MD)*: The thermistor depth (Inner or Outer) with the maximum magnitude – *i.e.* the most "active" depth for which the range of sap flux density is the largest (Link et al., 2014) – is chosen and kept constant across the length of the sapwood radius. Both thermistor depths are highly correlated – $R^2$ > 0.9 on average (data not shown), thus no information on the hourly dynamics of sap flux density is lost when using only one of the thermistor depths. For the focus tree, this approach resulted in the use of the Inner thermistor for all four azimuths.
- *Mean depths (AD)*: the inner and outer sap flux density measurements are averaged (Burgess and Downey, 2018)

**Zero-flow determination**: In theory, the HRM sensors should not require correcting for a zero-flow baseline. However, in practice, a small misalignment of the probes from improper installation or differential pressure exerted on the probes due to differential sapwood properties often lead to an offset in the zero in sap flux density measurements (Burgess and Downey, 2018). Determining a baseline sap flux density relative to zero flow conditions is a way to correct for that offset seen in practice when using the HRM sensors in the field. Several approaches are available to determine the zero-flow baseline in the literature from other types of sap flow sensors. Those approaches were individually tested to assess their impact on the precision of the sap flux estimates from the sap flow sensors (Rabbel et al., 2016). The first two, pre-dawn and study-specific approaches are commonly used in the literature for determining zero-flow (Burgess and Downey, 2018; Oishi et al., 2016, 2008). The regression methods are less commonly used but consider any temporal drift in the zero-flow measured by the sap flow sensors over time (Granier, 1987; Lu et al., 2004).

- *Pre-dawn correction (PD)*: commonly applied, this technique identifies the lowest daily sap flux density representing zero flow when environmental conditions are propitious for negligible water loss to the atmosphere and recharge of water above sensor height is negligible. We identified the lowest daily sap flux density for each sensor during the periods when solar radiation was less than 5 W $m^{-2}$ (nighttime), and the average minimum two hour VPD (vapor pressure deficit) was less than 0.05 kPa (Oishi et al., 2008) between July 19th and August 22nd, 2017. We thus obtained the average lowest hourly sap flux density during the night of 18 individual days during this period. Two calculations were then made. First, these individual lowest measurements of sap flux density were averaged to yield a unique value of pre-dawn sap flux density (PD). Second, a linear interpolation based on these individual average lowest measurements of sap flux density was performed, returning a complete daily series of lowest sap flux density measurements ($PD_d$). Each sensor's dataset was corrected for either PD or $PD_d$.
- *Study-specific environmental and experimental conditions (SS)*: when possible, zero-flow is determined following a cut made just below the sap flow sensors, effectively severing all flows (Burgess and Downey, 2018). In our study, sap flow towards the end of the experiment (days 10–12 after the initial cut) was near zero at night based on the direct gravimetric measurements, mimicking a cut directly under the sensor. We selected the nighttime (22:00–04:00) of the last two days (August 21st and August 22nd) as the reference for zero-flow for each sensor. Zero sap flux density was then defined as the average sap flux density measured for each sensor during that time interval.
- *Linear regression (LR)*: to overcome the potential issues of drifts in the data due to long-term installation of the sensors, and issues of nocturnal flow measurement, a linear regression of the lowest daily sap flux density identified over the whole length of the installation by a 10-day moving window is performed. The predicted lowest daily sap flux density from the linear regression is then used as daily zero-flow (Granier, 1987; Lu et al., 2004).
- *Double linear regression (DLR)*: This technique further refines the one above, by eliminating the data points above the regression line and performing a second regression on the restricted dataset (Lu et al., 2004).
- For all techniques, once zero-flow was estimated, the entire sap flux density dataset was corrected for the estimated zero sap flux density, either using a unique average value (PD and SS) or on a per-day basis ($PD_d$, LR and DLR) by subtracting the hourly sap flux density measurements with the calculated zero-flow baseline.

*Sapwood area measurements:* The conversion of corrected sap flux density $J_s$ to whole-tree sap flux ($Q$, L $hr^{-1}$) is a step where an introduction of bias is likely (Looker et al., 2016). Sap flux density is either assumed constant across the sapwood depth and multiplied by the measured sapwood area to obtain $Q$ or allowed to exhibit a radial pattern along with the sapwood depth. For the former option, the method used to determine sapwood depth and by extension sapwood area will modify the calculated estimates of sap flux rates. We assess the impact of the commonly used approximations of sapwood area and depth, as well as the use of a radial profile of sap flux density on the calculated estimates of sap flux rates. At each sensor location, tree disks were obtained to measure sapwood area and depth. For each disk the conductive sapwood was stained using a 0.0413% bromocresol green solution (Kutscha and Sachs, 1968). The samples were then scanned, and the total stained area or sapwood depth measured using scanning software ImageJ® (Schneider et al., 2012). Sapwood area was estimated as follows (for the three locations across the trunk below the canopy):

- *True sapwood area $SA_{true}$*: total sapwood area was measured for the disks sampled at each tree height.
- *One sapwood depth $SA_{tc;\,i}$*: using the tree disk, sapwood ($Sw_i$, *mm*) and heartwood depths ($Hw_i$, *mm*) to pith was measured at each sap flow sensor cardinal position at each height. Assuming a perfect annulus shape, the total sapwood area was calculated when measured from each cardinal direction ($SA_{tc;i}$).

$$SA_{tc;i} = \pi \times (Hw_i^2 - (Hw_i - Sw_i)^2)$$

- *Four sapwood depths averaged $SA_{tc;\,avg}$*: the measured sapwood and heartwood depths were averaged across cardinal positions. Assuming a perfect annulus, the total sapwood area was then calculated.

$$SA_{tc;avg} = \pi/4 \times (Hw_{avg}^2 - (Hw_{avg} - Sw_{avg})^2)$$

- *Two sapwood depths averaged*: the measured sapwood and heartwood depths from opposite ($SA_{tc;\,opp}$, N - S, E - W) and side-by-side cardinal positions ($SA_{tc;\,per}$, N - E, S - W, S - E, N - W) were averaged across cardinal positions and the total sapwood area was then calculated assuming a perfect annulus.

Sap flux $Q$ was calculated by multiplying the measured sap flux density from each cardinal direction by one of the four sapwood area estimates. In order to provide a first look at incorporating a more realistic description of the radial distribution of sap flux density along the sapwood length, sap flux was also calculated using a radial profile of sap flux density, specific to the diffuse-porous quality of the wood of trembling aspen (Berdanier et al., 2016).

### 2.6. Spatial variability between cardinal orientations and the use of single sap-flow sensors

Costs often limit the number of commercial sap flow sensors that can be installed in sap flux studies that could quantify the within-tree variability in sap flux rates (particularly on large trees) rather than only the between-tree variability. This might be very important for large trees where distinct microclimatic exposures, wood properties, or idiosyncrasies between cardinal aspects in the trunk may lead to different sap flux rates based on the position of the sap flow sensor. Extrapolating the measured sap flux rates on one cardinal aspect of the tree to the entire sapwood area, to the whole tree may lead to gross estimation errors of whole-tree sap flux rates and cumulative water volumes. To assess whether using multiple sensors would lead to more accurate estimates of whole-tree sap flux rates, we compared the use of single sensors with the use of four sensors placed at each cardinal direction (*i.e.*, north, south, east, and west), summed up to obtain whole-tree estimates with the scale data. For the purpose of these comparisons, we first corrected the sap flux density using the most commonly applied approaches, hence AD for radial integration method, PD for the zero-flow determination, and the best sapwood area measurement -

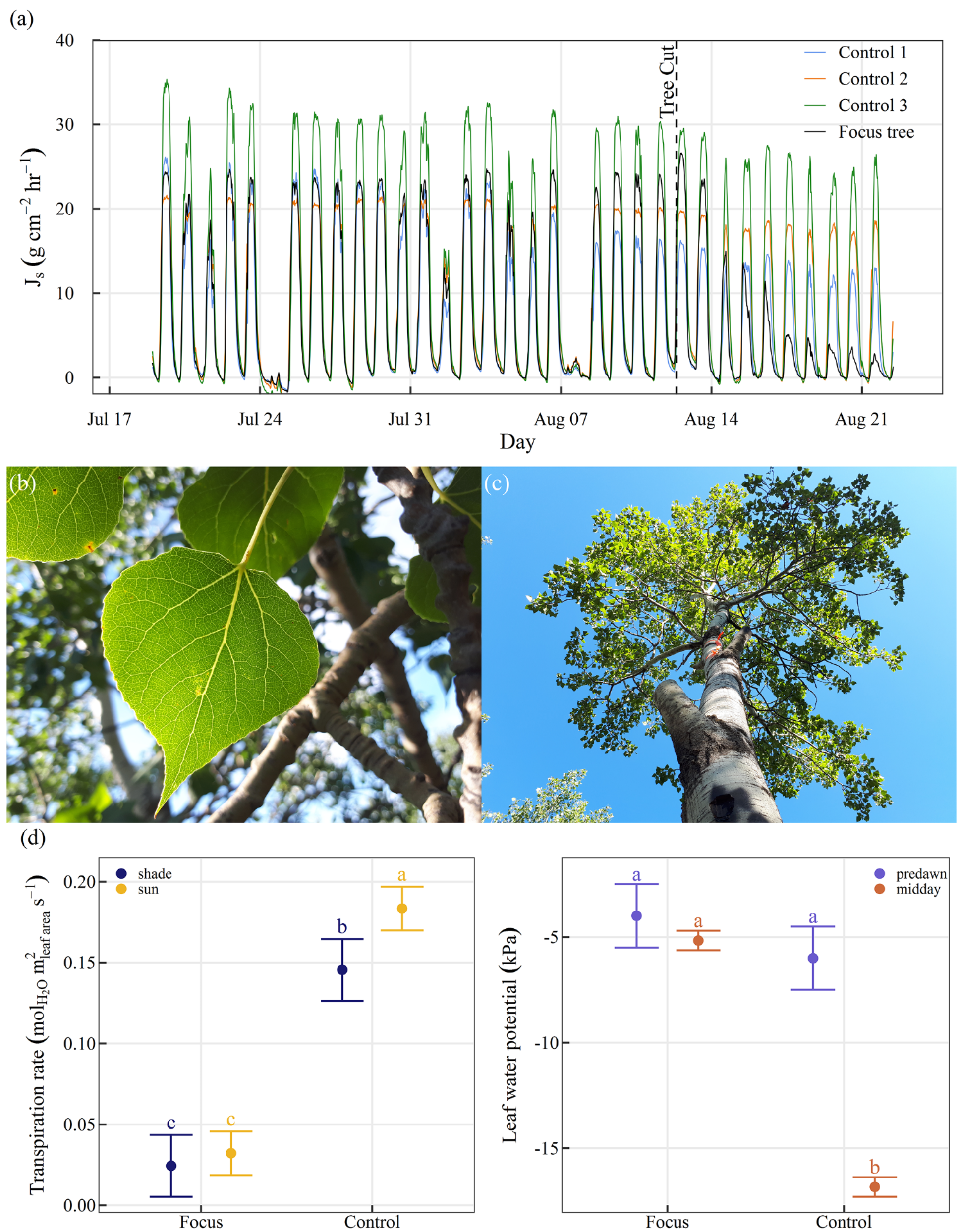


**Fig. 1.** Impact of the cut on the focus tree sap flux density and canopy health. Panel a shows the sap flux density $J_s$ (g $cm^2$ $hr^{-1}$, corrected using the PD zero-flow correction) at 30 min time intervals calculated on the north-facing sensor of the focus tree and three control trees between July 19th and August 22nd, 2017. The day the focus tree was cut is indicated by a vertical black dotted line with the label "Tree Cut" on August 12th, 2017. Panel b shows a single leaf from mid-canopy on August 17th (5 days after the cut). Panel c shows a view of the canopy on August 26th (14 days after cut, four days after the sap flow sensors were uninstalled from the focus tree and the lower branches removed). Panel d shows the leaf physiology described by transpiration rate (measured at midday on sun and shade leaves on days 4 and 8 after the cut), and leaf water potential (measured on sun leaves at midday on day 4 and predawn on day 8 after the cut) measured on the focus and control trees. Error bars represent 95% confidence intervals, and letters indicate statistical significance.

$SA_{true}$. The calculations were as followed, *for i in* $\{N, S, E, W\}$:

- *The use of single sensor extrapolated to the whole-tree*: the sap flux density measured at each cardinal direction is extrapolated to the entire sapwood area $SA_{true}$ to yield estimates of the whole-tree sap flux rates

$$Q_i = J_{s;i} \times SA_{true}$$

- *The use of four sensors*: the sap flux density measured at each cardinal direction is extrapolated to the sapwood area immediately surrounding the sensor location $SA_{true;i}$ (representing about a quarter of the total sapwood area $SA_{true}$) to obtain sap flux rates. The four cardinal sap flux rates are then summed up to obtain an estimate of whole tree sap flux rates.

$$Q_{quarter;\ i} = J_{s;\ i} \times SA_{true;i};\ Q_{quarter} = \sum_i Q_{quarter;\ i}$$

## *2.7. Statistical analysis*

All measurements of sap flux were aggregated into hourly intervals. We report sap flux density $J_s$ (g $cm^2$ $hr^{-1}$) and sap flux $Q$ (L $hr^{-1}$) measured from the sap flow sensors, and gravimetric water flux $Q_{scale}$ (L $hr^{-1}$) measured from the scale. Daily sap flux ($Q^d$, L $d^{-1}$) was calculated, as well as cumulative sap flux ($Q^c$, L) for both the sap flow sensors and the scale. We limit our analyses to the first five days after the cut (August 12th–16th, 2017) representing conditions most similar to before the cut.

*Physiology measurements:* Linear models were fitted on each of the canopy leaf transpiration rate and water potential measurements to test for the interaction between tree (focus *versus* control) and leaf type (shade *versus* sun) or measurement time (leaf water potential only, predawn *versus* midday).

*Spatial variability and temporal correlation:* We visually compared the single-sensor and four-sensors whole tree sap flux rates $Q_i$ and $Q_{quarter}$ against the gravimetric water uptake from the scale at the hourly timescale and in terms of cumulative water uptake. We assessed the temporal discrepancies between sensor-derived sap flux rates and the gravimetric scale data first by calculating the difference between the sap flux rates from both data sources rates during the daytime and nighttime (07:00–20:00), and across the seven days after the cut. Secondly, we fitted a linear model with a time series component between the hourly sensor-derived and scale sap flux rates using the function *tslm* from the *forecast* package in R (Hyndman et al., 2019). All of the following data analyses and statistical tests were done on the single-sensor derived sap flux rates, discarding $Q_{quarter}$.

*Zero-flow corrections and sapwood area estimation methods:* Linear mixed-effects models were used to test for the effect of radial integration method on the difference in the zero-flow correction estimates between PD and SS and on the slope of the relationship between $J_{s,\min}$ and time (Date) for $PD_d$. Additionally, a linear mixed-effects model was fitted on the slope between $J_{s,\min}$ and time (Date) defining LR and DLR to assess for differences between radial integration method and zero-flow method. Paired t-tests were used to assess whether the difference between the tree-core methods of sapwood area measurements ($SA_{tc}$, $SA_{tc\text{-}avg}$, $SA_{tc\text{-}opp}$, $SA_{tc\text{-}per}$, $SA_{tc\text{-}quarter}$) and $SA_{true}$ was significantly different from zero across trunk locations on the focus-tree.

*Calibration performance metrics:* Calibration performance was assessed using four dimensionless metrics assessing the performance of the data-processing procedures and cardinal orientation installation when comparing to the reference gravimetric scale data (Flo et al., 2019) over the first five days after the cut (August 12th–16th, 2017). All data points less or equal to zero were filtered out for the calculation of these metrics. The following metrics were calculated per day after the cut: the natural logarithm ratio ("Ln ratio") between the measured (*i.e.* sap flow sensor data) and reference scale water uptake as a measure of accuracy; the slope of the relationship between the measured and reference sap flux to represent proportional bias ("Slope"), as well as the slope of the ln-ln relationship to characterize linearity ("Slope (ln-ln)"), and the Z Pearson's correlation coefficient ("Z-correlation") to describe precision. Linear models were used to assess the differences in these calibration metrics between different zero-flow corrections and different sapwood area estimations for each cardinal direction separately. Three of the four calibration performance metrics declined progressively after the cut across cardinal orientations, even more so at night (data not shown). We chose to restrict our analyses to the first five days after the cut during the daytime (07:00–20:00) to assess the performance of the data-processing procedures for these calibration performance metrics. In that period, the four calibration metrics were relatively stable, and sap flux was most similar to before the cut and to the control trees (Fig. 1a, Fig. 2).

*Differences in cumulative water uptake estimates:* The absolute difference in cumulative water uptake over the first five days after the cut (August 12th–16th, 2017) between sensor-derived and scale water uptake measurements was calculated and linear models assessing the effect of cardinal orientation and the three data-processing procedures applied.

*Impact of the spatial variability and data-processing procedures on the relationship with climate:* We used all days before the cut with no precipitation and the first day after the cut (*i.e.* 27 days). The data from the subsequent days (August 13th–22nd, 2017) was not included, as the water flux through the cut-tree likely got disconnected from its climatic drivers. We assessed the relationship between sap flux and atmospheric VPD (kPa) at the hourly timescales using a modified logistic equation (Eq. (1)):

$$Q\ (L\ hr^{-1}) = \frac{Asymptote}{1 + e^{-steep\times(x-midpoint)}} + Constant \tag{1}$$

The equation parameters (Asymptote, Constant, Mid-point and Steep) were individually estimated for each combination of cardinal orientation, radial integration, zero-flow correction and sapwood area estimation. The effects of cardinal orientations and the three data-processing procedures were assessed using individual linear models on the asymptote, mid-point and steep parameters. The squared correlation between the fitted and observed values are reported as $r^2$ values. The same equation at the hourly timescale was used on the gravimetric scale data for the first two days after the cut to avoid introducing artificial bias resulting from the decline in sap flow induced by the cut-tree method by including days 3 to 10 after the cut.

All statistical analysis were performed using the R statistical software v3.5.1. (R Development Core Team, 2019). All the analyses were performed using linear models or linear mixed-effects models with the package *nlme* (Pinheiro et al., 2018). Normality and homoscedasticity assumptions were checked for all models, and corrections applied when necessary. Models specifics and summary statistics (degrees of freedom, sample size, test statistic, coefficient of determination) are also provided in the Supplementary Material B. Estimated marginal means and 95% confidence intervals were calculated using the package *emmeans* (Lenth, 2018) to summarize the effects of the fixed factors ($\alpha = 0.05$). The coefficient of determination $r^2$ is reported for linear models and the marginal and conditional $r^2$ for mixed effects models.

## 3. Results

### 3.1. Sap flow response to the cutting

Immediately after the cut and for the next 48 h, sap flux density ($J_s$) was similar to measurements taken before the cut and to those measured in the three control trees (Fig. 1a). Sap flux density then declined in the focus tree over the next eight days compared to the three control trees, which all maintained higher $J_s$. Interestingly the crown of our focus tree showed no sign of hydraulic damage for the duration of the study (*i.e.* wilting or color changes; Fig. 1b and c). Transpiration rate of the focus tree after the cut was about 20 − 30% of the transpiration rate of the control trees (Fig. 1d). Shoot water potential at pre-dawn was slightly higher (less negative) than the control, indicating ample water supply over the ten days after the cut, this response became more apparent during midday when shoot water potentials were somewhat lower in the focus tree, but dropped by more than 10 kPa in the control trees (Fig. 1d).

### 3.2. Spatial variability in sap flow sensor location between cardinal aspects

Using standard data-processing procedures (AD, PD, and $SA_{tc}$), the agreement of the sap flux with the gravimetrically measured $Q_{scale}$ was variable and heavily depended on the cardinal position of the sensor on the trunk (Fig. 2a). Summing up the sap fluxes calculated at each cardinal orientation into $Q_{quarter}$ did not improve or worsen the fit with the gravimetric data (Fig. 2b). The difference between the scale and sensor sap flux rates was lowest during high flow periods (*i.e.* the first four days after the cut and during the day). The higher discrepancies between the scale and the sensors sap flux rates particularly at night might have been due to the relatively low precision of the scale (0.2 L $hr^{-1}$). However, the temporal correlation of $Q_i$ and $Q_{quarter}$ with $Q_{scale}$ was high, with no time lag between the two (data not shown, $R^2 = 0.99$). Cumulative water uptake over the five days after the cut was 191.2 L from the scale data. Using those standard data-processing procedures (AD, PD, and $SA_{tc}$), the cumulative water uptake estimates using single sensors ranged between 124.1 L (south-facing sensor) to 209.7 L (north-facing sensor). Using the sum of the cardinal fluxes yielded an estimate of 178.9 L.

### 3.3. Zero-flow determination approaches and sapwood area calculations

The zero-flow $J_{s,\min}$ strongly depended on the correction method and varied between cardinal orientations and radial integration method used (Supplementary Material Fig. C.1a). Under the PD correction, $J_{s,\min}$ was higher than under the SS correction (mean difference:

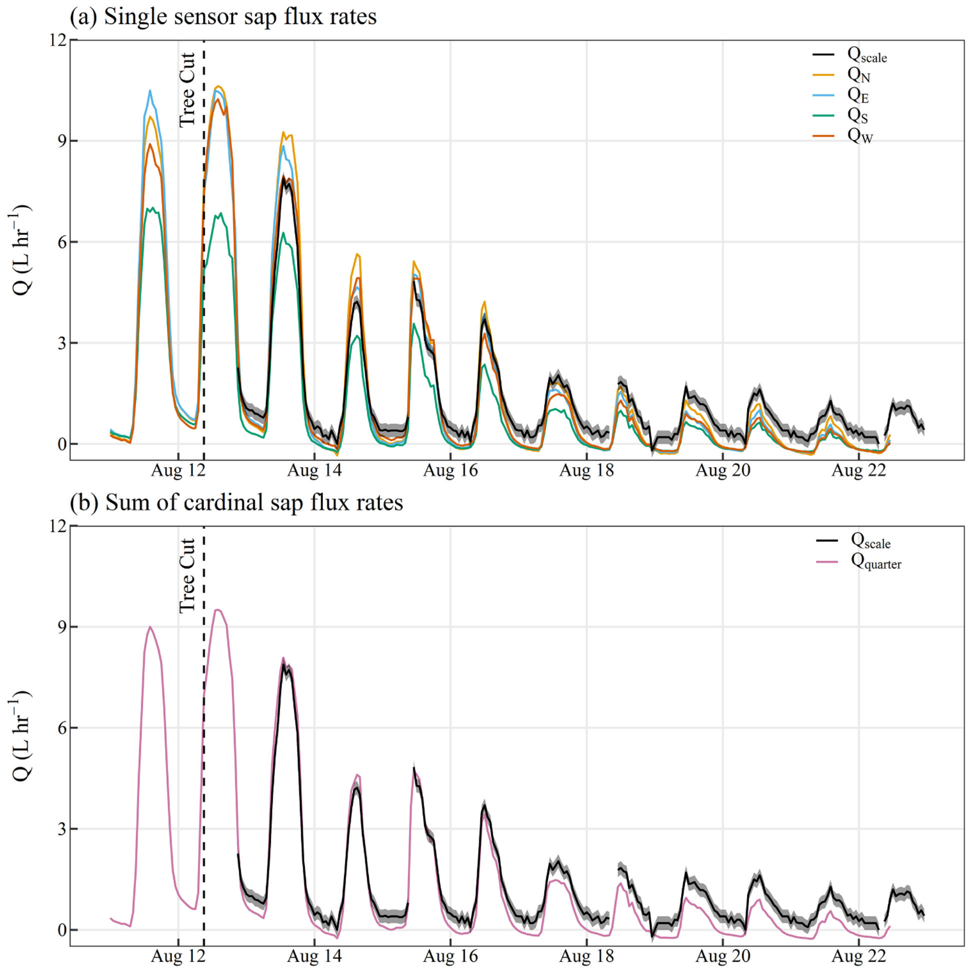


**Fig. 2.** Comparison between the individual sensor-measured and scale hourly sap flux rates. The scale sap flux rate is shown in black, with its 0.2 L $hr^{-1}$ precision as gray shaded area. Panel a shows single sensor sap flux rates $Q_i$ for each cardinal orientation i. Panel b shows the sap flux rates calculated as the sum of the cardinal fluxes, $Q_{quarter}$. All sensor-derived sap flux rates were calculated using the AD radial integration, PD zero-flow determination and $SA_{tc}$ for the sapwood area calculation, with $n = 1$.

0.420 g $cm^2$ $hr^{-1}$), more so with AD than with MD (difference estimate: AD = 0.544 g $cm^2$ $hr^{-1}$; MD = 0.296 g $cm^2$ $hr^{-1}$) (Supplementary Material Table B.1). Under the $PD_d$ correction $J_{s,\min}$ significantly declined over 30 days, marginally more so with AD than MD (slope estimate: AD = −0.047 [−0.055; −0.039]; MD = −0.037 [−0.045; −0.029]), however, most of the variation was explained by the sensor cardinal placement. The slope in the defining regression of the LR and DLR corrections was overall not significantly different from 0 but largely varied between cardinal orientations and radial integration method used.

None of the tree-core derived estimates of sapwood area were significantly different from $SA_{true}$ (Supplementary Material Table B.2). Using $SA_{tc\text{-}quarter}$ or $SA_{tc\text{-}avg}$ yielded the lowest deviation from the $SA_{true}$, followed by $SA_{tc;\text{-}per}$, then $SA_{tc\text{-}opp}$. Using $SA_{tc}$ resulted in a large variation across trunk heights and cardinal direction, with up to 60 $cm^2$ difference with $SA_{true}$ (Supplementary Material Fig. C.1b).

### 3.4. Impact of the data-processing methods on the accuracy of the sap flux rates

#### 3.4.1. Hourly estimates

The cardinal placement of the sensor and data-processing procedures applied to the data set significantly influenced the calibration performance metrics (Fig. 3). Accuracy and linearity were closest to the reference for the north, and west orientations; however, proportional bias was lowest for the east and south orientations. Precision was highest for the north orientation. The use of the MD radial integration method showed a larger proportional bias but better accuracy than AD, with similar linearity and precision. Regarding the zero-flow corrections, the linear regression methods LR and DLR showed the highest accuracy and linearity, followed by the SS correction. The use of a radial profile decreased accuracy but improved the proportional bias compared to the other sapwood area estimation methods. None of the data-processing procedures showed any significant differences in precision. The integration of the four cardinal measurements of sap flux rates into $Q_{quarter}$ improved proportional bias for the AD radial integration method (0.99 [0.97; 1.01]) and slightly increased the precision but did not lead to an overall improvement of the accuracy and linearity (Supplementary Material Fig. C.2).

#### 3.4.2. Cumulative estimates

Over the five days after the cut, the hourly discrepancies between the gravimetric scale and the single-sensor sap flux rates cumulated to differences that ranged from less than 1 L to near 125 L in the final cumulative water uptake tally, with a significant interaction between sensor placement and data-processing procedures (Fig. 4a). Using MD significantly decreased the deviation from the gravimetric cumulative water uptake compared to AD when a sensor was positioned on the south (and marginally on the east) side of the trunk, but the deviation increased for the north and west positions. The SS, PD and $PD_d$ zero-flow corrections produced a deviation of 25 L or less on average from the gravimetric cumulative water volume (Fig. 4b). The use of R, $SA_{tc}$

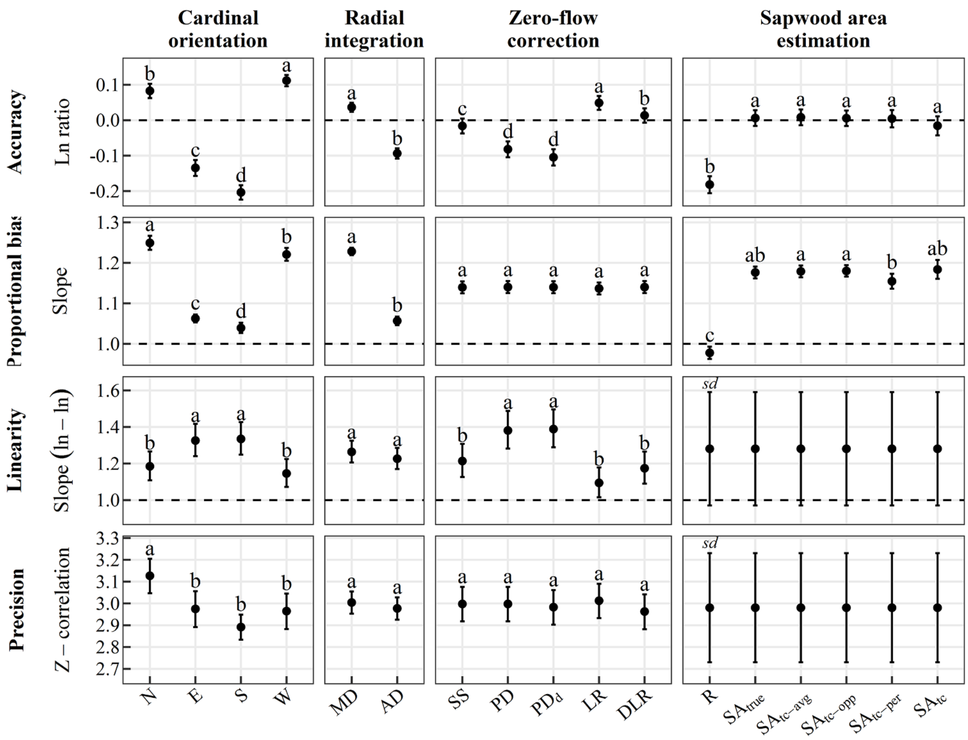


**Fig. 3.** Summary of the calibration performance metrics for the azimuthal sensor placement and the different methods applied in the three data-processing procedures (radial integration, zero-flow correction, and sapwood area estimation). The metrics were estimated during the daytime (07:00–20:00) the first four days after the cut. Means and 95% confidence intervals are shown. Different letters indicate significant differences across data correction procedures (Supplementary Material Table B.3). Note that for the slope (ln-ln) and the Z-correlation for the sapwood area estimation variable, the values were identical across the different methods; hence the figure shows mean and standard deviation ("sd" label). Horizontal dotted lines indicate reference value, for a perfect calibration value for each metric. The intersection between the confidence interval and the reference line indicates that the metric is not significantly different from the reference. Data distribution of the calibration performance metrics across the azimuthal sensor placement and the three data-processing procedures is shown in Supplementary Material Fig. B.1.

and $SA_{tc-per}$ sapwood area estimation methods produced larger differences with the gravimetric cumulative water volume (Fig. 4b). Integrating the four aspects into a single whole-tree cumulative sap flux resulted in a smaller deviation from the gravimetric measurements, ranging between 10 and 30 L on average, with no differences between radial integration, zero-flow and sapwood area estimation approaches (Supplementary Material Fig. C.2).

Nighttime cumulative water uptake represented 20% and 10% of the total daily volume from the gravimetric and sensor measurements respectively (*i.e.* 53.1 L and 26.6 L respectively, results not shown). The sensor estimates were slightly higher before the tree was cut (13% of total cumulative sap flux).

*3.4.3. Consequences of correlating sap flux rates with climatic drivers*

All data-processing procedures showed a very good fit with hourly VPD, with little difference between the best and worst fits in terms of $r^2$ (Fig. 5). No differences in the strength of the fit were found among the different sapwood area estimates, as they only differed by a multiplicative factor. The gravimetric data showed a lower asymptote, higher mid-point and higher steepness estimates than most of the data-processing procedure combinations (Fig. 5, Table 1). The cardinal orientation and radial integration explained most of the variation in the parameters of the logistic relationship between hourly sap flux and VPD (Table 1, Supplementary Material Table B.4). The asymptote and mid-point were significantly higher when MD while the opposite was true for the steepness parameter. All zero-flow determination approaches yielded very similar parameter estimates; however, the LR and DLR had a lower mid-point and steepness parameters than the other corrections. Only the use of the radial profile differed from the other sapwood area estimation methods, with a lower asymptote (Table 1, Supplementary Material Table B.4).

A summary of the results comparing the sap flow sensor data and the gravimetric scale data using the different categories of descriptors is presented in Table 2. Cardinal orientation and radial integration often had the most considerable effect on the descriptors, while the zero-flow corrections and sapwood area estimation methods had a subtler effect. For each data-processing procedure, no best method clearly appeared across all descriptors, except for the SS zero-flow correction and the north orientation which seemed to perform slightly better on the majority of descriptors than other approaches.

## 4. Discussion

We quantified the uncertainties introduced by the placement of sap flow sensors (cardinal directions) and the application of different data-processing approaches (radial integration method used, zero-flow correction, and sapwood area estimation methods) on sap flow estimates for large diameter trees. These estimates were compared to gravitational measurements using the cut-tree method. The temporal precision of sensor-derived fluxes with the gravimetrically-measured water uptake was high when estimated across the different cardinal orientations and data-processing approaches for the HRM sensors. Almost all data-processing procedures showed a positive proportional bias, unlike previous studies reporting negative proportional bias (Flo et al., 2019; Fuchs et al., 2017). The limited range of sap flux densities in our study likely precluded the commonly reported saturation effect of the HRM responsible for the previous studies' results. Altogether, the choice of azimuthal placement of the sensor and the choice of data-processing approach resulted in a broad range of cumulative water uptake estimates over a short period of five days.

*Most sap flow measurement errors are related to azimuthal and radial variability of sap flux density*

Despite the visual symmetry of the focus tree and its sapwood area, the cardinal placement of the sensors and the radial integration method used had a significant impact on the sensor-derived sap flux rates. These two factors had the largest effect on the sensor's accuracy, proportional bias, and precision. A relatively small number of studies have considered azimuthal variations in sap fluxes, finding them related to structural anatomy and wood properties (López-Bernal et al., 2010), microclimatic conditions (Zhang et al., 2018), and seasonal variation (Chiu et al., 2016). No systematic pattern across and within species and studies have appeared so far (Sato et al., 2012; Van de Wal et al., 2015). In this study, the north-facing sensor seemed to perform slightly better than all other orientations across the performance descriptors in comparison with the gravimetric measurements, which we speculate may due to the lower influence of natural temperature gradients on the

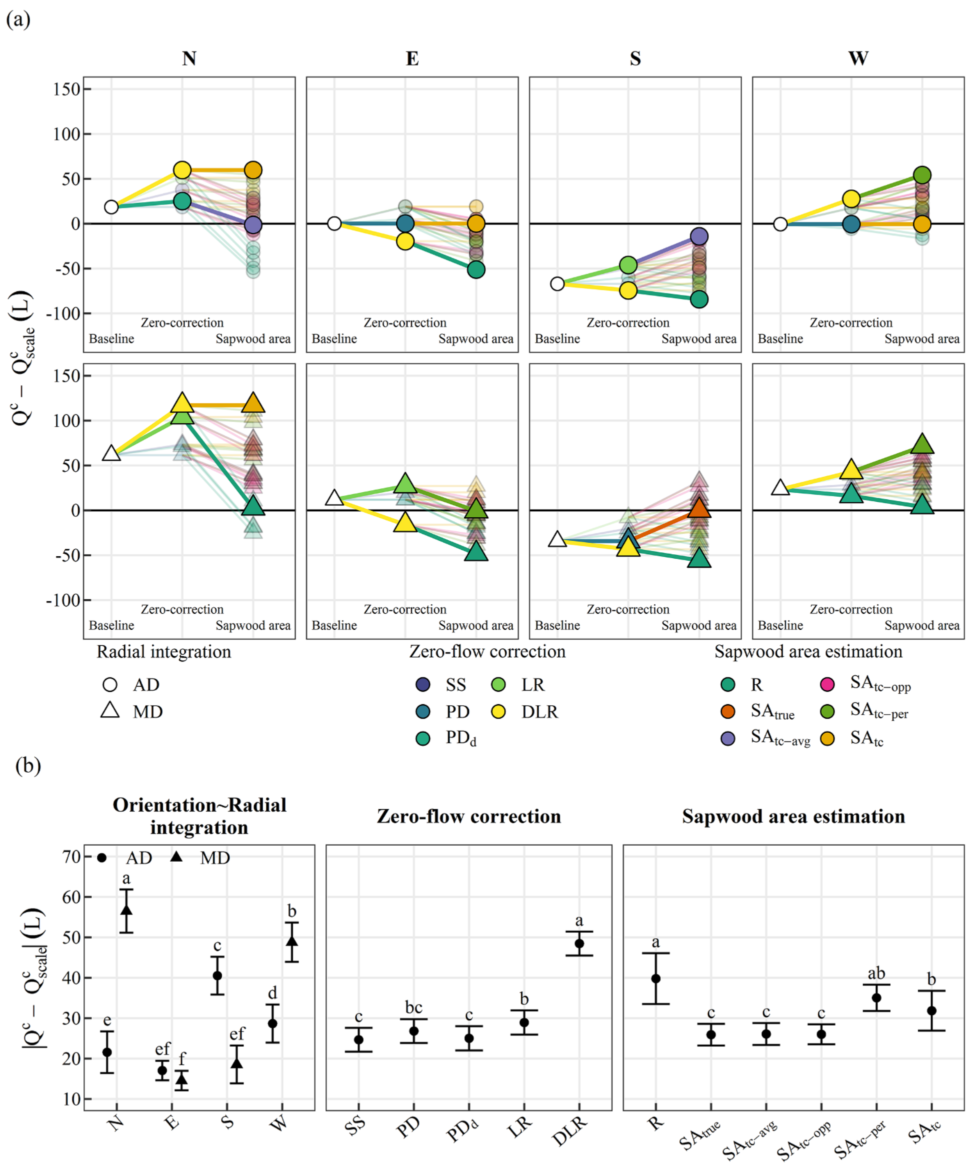


**Fig. 4.** Difference between sensor ($Q^c$) and gravimetric ($Q^c_{scale}$) estimates of cumulative water uptake over the five days after the cut for cardinal placement of the sap flow sensor and the three data-processing procedures. Panel a presents all data-processing combinations, highlighting the best (closest to zero) and worst (farthest from zero). Baseline: PD and $SA_{tc}$. We show how the use of different zero-flow corrections alter the cumulative water uptake estimate from the Baseline ("Zero-correction"), followed by the use of different sapwood area calculation methods ("Sapwood area"). Panel b shows the mean and 95% confidence interval in the estimate of the absolute difference between the sensor and gravimetric cumulative water uptake for the interaction between the cardinal placement of the sensor and radial integration approach, zero-flow correction and sapwood area estimation methods. Letters indicate statistical differences.

sensor measurements of sap flux density (Vandegehuchte et al., 2015, not the scope of the study). Integrating sap flux measurements among the four cardinal positions instead of using single-position measurements did not generally improve the calibration performance metrics results but significantly decreased the deviation in the estimate of whole-tree cumulative water uptake in the first five days before the cut. The inclusion of the azimuthal aspect in any future sap flow experiment should be carefully considered (Tseng et al., 2017), especially for large trees with a higher probability of azimuthal variability in sap fluxes and when a limited number of sap flow sensors is available (Komatsu et al., 2017). An initial pilot study assessing whether there is a basis for strong environmentally-driven circumferential variability in sap flow in individual trees in a stand would help improve the decision-making process in the sensor allocation, to integrate or ignore this within-tree circumferential variability in water uptake.

Radial patterns of sap flux density within the sapwood have an equally significant impact on whole tree sap flux estimation. Sap flux density measurements from the two thermistors of the HRM sensors are highly correlated but display a different range of sap flux density measurements following their positioning at different sapwood depths. Arguments have been made to use the thermistor depth with the maximum magnitude of measurements to focus on the "most functioning" xylem depth, especially when relating to environmental variables such as VPD (Link et al., 2014). However, this can potentially overestimate sap flux rates when extrapolating to whole-tree estimates. Using MD increased the proportional bias in hourly sap flux and the deviation from the gravimetric measurements of cumulative water uptake for the north and west aspects only, highlighting an interactive effect between azimuthal and radial variability of sap flux density (Lu et al., 2004; Zhang et al., 2018). Most of our results are inconclusive regarding the use of MD or AD for our study tree. Integrating multiple point measurements over a species-specific radial profile of sap flux density could significantly improve the performance of the sap flow sensors (Hernandez-Santana et al., 2015). The coarse application of a diffuse-porous radial profile (Berdanier et al., 2016) to our dataset showed overall mixed results. Proportional bias was reduced, but accuracy decreased substantially, and the absolute difference with gravimetric cumulative water volume was the highest across sapwood area estimation methods. A proper calibration of the radial profile equation for this species and other large-diameter trees using multi-sensor needles across the sapwood depth would likely improve our results (Forster, 2017; Hatton et al., 1990; Wullschleger and King, 2000) but is often not feasible when using costly commercially available sap flow sensors. In the absence of information regarding the

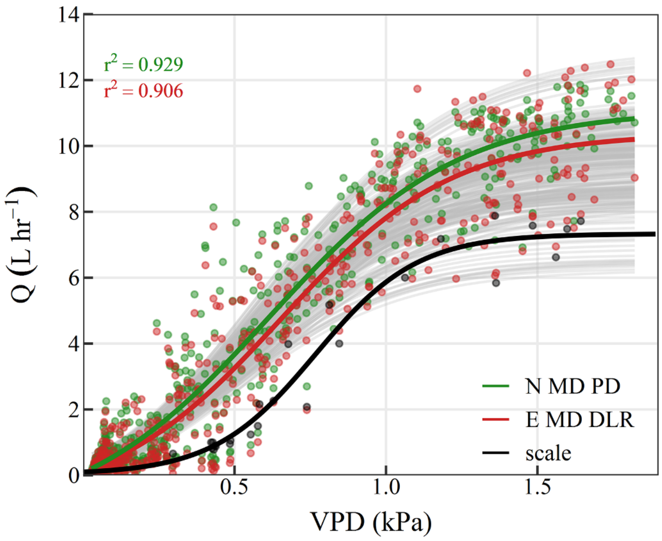


**Fig. 5.** Hourly measured (points) and modelled logistic relationship (line) between hourly sap flux rates (hourly) and atmospheric VPD for each combination of the sensor cardinal placement and data-processing procedures (light gray) and for the scale gravimetric flux (black). The individual relationships with the best (green) and worst (red) fit ($r^2$) are shown, and the combination explicit in the legend (cardinal orientation ~ radial integration ~ zero-flow correction) for each panel. The sapwood area estimation is not explicit as it did not have an impact on the fit. (For interpretation of the references to color in this figure legend, the reader is referred to the web version of this article.)

radial profile of sap flux density, extrapolating constant sap flux density across $SA_{true}$ or $SA_{tc\text{-}avg}$ and $SA_{tc\text{-}opp}$ showed the best results.

*Differences in sap flux estimation caused by zero-flow corrections*

The five different zero-flow corrections tested in the study were in the range of 0–2 g cm$^2$ s$^{-1}$, similar to what has been reported previously (Rabbel et al., 2016). The environmentally-defined pre-dawn zero flow corrections (PD and $PD_d$) showed the lowest scores in accuracy and linearity, unexpectedly, considering this type of correction has been highlighted as the most likely to yield the best zero-flow estimation (Oishi et al., 2008; Peters et al., 2018; Rabbel et al., 2016). Significant nocturnal sap flux (representing 20% of total daily cumulative sap flux in this large aspen tree) or the influence of stem water storage dynamics may have contributed to this result in our focus tree (Peters et al., 2018). When the application of the well-performing SS correction is not available, the linear regression techniques performed best in terms of accuracy and linearity, although the use of the DLR led to the highest absolute difference in cumulative water uptake. It has been hypothesized that zero-flow conditions may develop over time, and the use of more static methods such as PD and SS could lead to increasing discrepancies (Rabbel et al., 2016), hence the use of the regression techniques. It is, however, possible that over an extended time period linear regression methods may not fare as well, as changes in phenology, wood thermal properties, and climatic conditions may trigger non-linear changes in minimum sap flux densities (Peters et al., 2018; Rabbel et al., 2016; Vergeynst et al., 2014). The zero-flow determination, though not as crucial for the heat pulse velocity sap flow sensors as for other sensor families, remains a data-processing step for which there is little consensus as to which to use. To our knowledge, no study has yet been able address the issue of potential evolution of the zero-flow baseline during an entire experiment while accurately and directly measuring instances of null flow.

*Implications for correlating sap flux with climatic variables and for stand-level transpiration estimates*

All sensor cardinal positions and data-processing approaches showed very high correlation ($R^2 > 0.9$) with atmospheric VPD, showing a high consistency regardless of the position and correction method chosen, unlike what has been found in other studies (Peters et al., 2018; Rabbel et al., 2016). Sensor position and the variability in sap flux estimates with sapwood depth significantly affected the parameters defining the hourly relationship with VPD, showing a significant departure from the gravimetric data. All sensor cardinal orientations and data-processing methods largely overestimated the asymptote, *i.e.* maximum water use rate at high VPD, and underestimated the mid-point and steepness parameters compared to the relationship based on gravimetric measurements. Although the dataset used to derive the latter was restricted to only two days, this result highlights that the modeled dynamics between VPD and sensor-based sap flux rates may not be fully representative of large tree's behaviors. Deriving estimates of canopy conductance and water usage in response to climatic variables based on sap flux measurements is a common approach, but as highlighted here, decisions such as the placement of the sap flow sensors or the choice of data-processing approach may lead to significant discrepancies that impact the interpretation of responses to changes in VPD. Those seemingly small differences at the individual tree scale accumulate significantly when upscaled spatially and temporally. Over only five days, we saw total cumulative water uptake misestimated between 1 to more than 50%. This uncertainty will most likely increase when considering an entire growing season, and when upscaling water use from a single tree to a stand- or landscape-level (Čermák et al., 2004; Peters et al., 2018). Deliverables from sap flux studies (*e.g.* their relationships with climatic and environmental variables and their extrapolation of cumulative water volumes transpired by forests) play a significant role in current vegetation models and forest and land management decisions. Considering the critical questions these models address (forest productivity and mortality, species distribution, hydrological cycling, and climate change impacts) it becomes necessary to assess in more detail and

**Table 1**
Mean and 95% confidence intervals of the parameters of the logistic relationship between hourly gravimetric (scale) and sensor-based sap flux rates and VPD (Asymptote, mid-point and steepness; rows). The means and 95% confidence intervals obtained from the models assessing the effects of the sensor placement and the three data-processing procedures are shown for each parameter (columns). Letters indicate significant differences between methods for each data-processing procedures. As all zero-flow determination approaches yielded very similar estimates, they are summarized in a unique value. The same is applied for all the sapwood area estimation methods ($SA_{true}$, $SA_{tc\text{-}avg}$, $SA_{tc\text{-}per}$, $SA_{tc\text{-}opp}$ and $SA_{tc}$ summarized in $S_{all}$) but R. Mean and standard deviation (sd) are presented for the mid-point and steepness for the sapwood area estimation as the values were identical.

| | Scale | Sensor Orientation | | | | Radial integration | | Zero-flow approach | Sapwood area estimation | |
|---|---|---|---|---|---|---|---|---|---|---|
| | | N | E | S | W | AD | MD | All | R | $SA_{all}$ |
| Asymptote | 7.31 | 11.25<br>[10.85;11.64] ab | 10.98<br>[10.79;11.17] b | 9.39<br>[9.1;9.68] c | 11.24<br>[11.06;11.41] a | 10.21<br>[10.05;10.38] b | 11.21<br>[11.02;11.41] a | 10.69<br>[10.47;10.91] | 9.22<br>[9.04;9.42] b | 10.98<br>[10.71;11.25] a |
| Mid-point | 0.77 | 0.57<br>[0.56;0.58] c | 0.61<br>[0.6;0.62] a | 0.6<br>[0.6;0.6] b | 0.56<br>[0.53;0.59] c | 0.52<br>[0.5; 0.53] b | 0.63<br>[0.63;0.64] a | 0.59<br>[0.58;0.59] | 0.58<br>[sd: 0.05] | |
| Steep | 5.95 | 3.38<br>[3.37;3.4] c | 3.77<br>[3.76;3.78] b | 3.84<br>[3.83;3.86] a | 3.38<br>[3.35;3.41] c | 3.8<br>[3.79;3.81] a | 3.38<br>[3.37;3.39] b | 3.59<br>[3.58;3.61] | 3.59<br>[sd: 0.3] | |

**Table 2**
Summary of the best cardinal orientation, radial integration method, zero-flow correction and sapwood area estimation for the three following categories: calibration performance metrics (Flo et al., 2019) (accuracy, proportional bias, linearity, and precision), correlation with VPD (kPa, hourly and daily) and cumulative water uptake. For the first and third categories, the sap flow sensor data is compared to the gravimetric scale data. For the relationship with VPD, the factor levels for which the parameters were closest to the gravimetric parameters of the logistic relationship between sap flux and VPD are shown. When no significant differences were found between methods, "NA" is displayed.

| | Calibration performance metrics | | | | VPD relationship | Cumulative water uptake |
|---|---|---|---|---|---|---|
| | Accuracy | Proportional bias | Linearity | Precision | Closest to gravimetric parameters | |
| Orientation | N | S | N; W | N | S | W |
| Radial integration | MD | AD | *NA* | *NA* | AD | *NA* |
| Zero-flow correction | SS; DLR | *NA* | SS; LR; DLR | *NA* | *NA* | SS; PD; $PD_d$; |
| Sapwood area estimation | All but R | R | *NA* | *NA* | R | $SA_{true}$, $SA_{tc\text{-}avg}$; $SA_{tc\text{-}opp}$ |

across sap flow sensor families how different methodological steps impact our current and future understanding and interpretation of water flow in trees and their extrapolation to various spatial and temporal scales (Ward, 2016).

## 5. Conclusion

This cut-tree study of sap flux measurements on a large mature tree using the HRM sap flow sensors highlighted that uncertainties arise from several methodological steps from sensor installation to the calculation of hourly sap fluxes. Although the cut-tree method provides a unique way to directly obtain gravimetric measurement of water uptake at a fine temporal scale for large trees (Olbrich, 1991; Roberts, 1977; Smith, 1992; Vertessy et al., 1997), these studies are complex to set up and present disadvantages and limitations. The separation of the crown and stem from the root system and the total immersion of the stem surface in water have contributed to the steady decline of sap flux density we observed in our study (beyond the scope of this paper). Conducting parallel experiments, using the weighing lysimeter and cut-tree methods may contribute to filling in the gaps in our interpretation of the observed decline in sap flux rate signals seen in this study, strengthening the conclusions drawn on the appropriate data-processing procedures to reduce uncertainties in sap flux rates in large trees. Nonetheless, we showed that for this large mature aspen tree, placing the sap flow sensors on the north-facing side of the tree, using either the LR or SS zero-flow correction and using tree disks or a minimum of two opposing tree-cores to estimate sapwood area were the best choices for increased accuracy with the gravimetric data. This study highlights the need for systematic and explicit handling of uncertainties in sap flow studies. Further comprehensive testing of the impact of sensor placement and the choice of data-processing methods on sap flux estimates is required to obtain a comprehensive handbook guiding the best available practices for using different families of sap flow sensors in trees of varying diameter and wood properties. It will eventually improve our understanding of tree water use at different spatial and temporal scales.

## CRediT authorship contribution statement

**Morgane Merlin:** Conceptualization, Methodology, Investigation, Formal analysis, Visualization, Writing - original draft. **Kevin A. Solarik:** Conceptualization, Methodology, Investigation, Writing - review & editing. **Simon M. Landhäusser:** Funding acquisition, Project administration, Supervision, Conceptualization, Methodology, Investigation, Writing - review & editing.

## Data for reference

The data and computer code that support the findings of this study will be available on the Dryad Repository.

## Declaration of Competing Interest

The authors declare that they have no known competing financial interests or personal relationships that could have appeared to influence the work reported in this paper.

## Acknowledgments

We thank Ian Jamieson for his invaluable help and expertise during planning and construction of the wooden structure, as well as Peter Lazowski for his help in the field. We thank all those who provided field and logistical support for this project (Frances Leishman, Robert Hetmanski, Natalie Scott, Ashley Hart, and Julie Zettl) as well as laboratory work (Pak Chow) and data-processing support (Newton Tran, ICT International Pty Ltd.). We thank Cinnamin Landhäusser for her support and motivation in the field. This work was supported by provided by the Natural Sciences and Engineering Research Council (NSERC), the Canadian Oil Sands Innovation Alliance (COSIA, Syncrude Canada Ltd., Canadian Natural Resources Ltd., Suncor Energy, Imperial Oil Ltd.) and TransAlta Corporation (grant NSERC/COSIA/TransAlta Industry Research Chair IRCPJ 378901-2013). The authors also acknowledge the constructive comments and suggestions of two anonymous reviewers.

## Supplementary materials

Supplementary material associated with this article can be found, in the online version, at doi:10.1016/j.agrformet.2020.107926.

## References

Alberta Climate Information Service (ACIS), 2018. Interpolated weather data since 1961 for Alberta townships [WWW document]. URLhttps://agriculture.alberta.ca/acis/alberta-weather-data-viewer.jsp(accessed 9.10.17).
Berdanier, A.B., Clark, J.S., 2018. Tree water balance drives temperate forest responses to drought. Ecology 99, 2506–2514. https://doi.org/10.1002/ecy.2499.
Berdanier, A.B., Miniat, C.F., Clark, J.S., 2016. Predictive models for radial sap flux variation in coniferous, diffuse-porous and ring-porous temperate trees. Tree Physiol. 36, 932–941. https://doi.org/10.1093/treephys/tpw027.
Bleby, T.M., Burgess, S.S.O., Adams, M.A., 2004. A validation, comparison and error analysis of two heat-pulse methods for measuring sap flow in *Eucalyptus marginata* saplings. Funct. Plant Biol. 31, 645. https://doi.org/10.1071/FP04013.
Bonan, G.B., 2008. Forests and climate change: forcings, feedbacks, and the climate benefits of forests. Science 320 (80–.).), 1444–1449. https://doi.org/10.1126/SCIENCE.1155121.
Burgess, S.S.O., Adams, M.A., Turner, N.C., Beverly, C.R., Ong, C.K., Khan, A.A.H., Bleby, T.M., 2001. An improved heat pulse method to measure low and reverse rates of sap flow in woody plants. Tree Physiol. 21, 589–598. https://doi.org/10.1093/treephys/21.9.589.
Burgess, S.S.O., Downey, A., 2018. SFM1 Sap Flow Meter Manual. ICT International Pty Ltd, Armidale, NSW, Australia.
Čermák, J., Kučera, J., Nadezhdina, N., 2004. Sap flow measurements with some thermodynamic methods, flow integration within trees and scaling up from sample trees to entire forest stands. Trees 18, 529–546. https://doi.org/10.1007/s00468-004-0339-6.
Chiu, C.-W., Kume, T., Komatsu, H., Tseng, H., Wey, T.-H., Otsuki, K., 2016. Seasonal changes of azimuthal, radial, and tree-to-tree variations in sap flux affect stand transpiration estimates in a *Cryptomeria japonica* forest, central Taiwan. J. For. Res

21, 151–160. https://doi.org/10.1007/s10310-016-0525-6.
Cohen, Y., Cohen, S., Cantuarias-Aviles, T., Schiller, G., 2008. Variations in the radial gradient of sap velocity in trunks of forest and fruit trees. Plant Soil 305, 49–59. https://doi.org/10.1007/s11104-007-9351-0.
Doody, T.M., Colloff, M.J., Davies, M., Koul, V., Benyon, R.G., Nagler, P.L., 2015. Quantifying water requirements of riparian river red gum (*Eucalyptus camaldulensis*) in the Murray-Darling basin, Australia - implications for the management of environmental flows. Ecohydrology 8, 1471–1487. https://doi.org/10.1002/eco.1598.
Fernández, E., Čermák, J., Cohen, Y., Ferreira, I., Nadezhdina, N., Testi, L., Steppe, K., 2017. Methods to estimate sap flow, in: ISHS Working Group On Sap Flow. pp. 1–9.
Flo, V., Martinez-Vilalta, J., Steppe, K., Schuldt, B., Poyatos, R., 2019. A synthesis of bias and uncertainty in sap flow methods. Agric. For. Meteorol. 271, 362–374. https://doi.org/10.1016/J.AGRFORMET.2019.03.012.
Forster, M.A., 2017. How reliable are heat pulse velocity methods for estimating tree transpiration? Forests 8, 350. https://doi.org/10.3390/f8090350.
Fuchs, S., Leuschner, C., Link, R., Coners, H., Schuldt, B., 2017. Calibration and comparison of thermal dissipation, heat ratio and heat field deformation sap flow probes for diffuse-porous trees. Agric. For. Meteorol. 244–245, 151–161. https://doi.org/10.1016/J.AGRFORMET.2017.04.003.
Granier, A., 1987. Evaluation of transpiration in a Douglas-Fir stand by means of sap flow measurements. Tree Physiol. 3, 309–320. https://doi.org/10.1093/treephys/3.4.309.
Hassler, S.K., Weiler, M., Blume, T., 2018. Tree-, stand- and site-specific controls on landscape-scale patterns of transpiration. Hydrol. Earth Syst. Sci. 22, 13–30. https://doi.org/10.5194/hess-22-13-2018.
Hatton, T.J., Catchpole, E.A., Vertessy, R.A., 1990. Integration of sapflow velocity to estimate plant water use. Tree Physiol. 6, 201–209. https://doi.org/10.1093/treephys/6.2.201.
Hernandez-Santana, V., Hernandez-Hernandez, A., Vadeboncoeur, M.A., Asbjornsen, H., 2015. Scaling from single-point sap velocity measurements to stand transpiration in a multispecies deciduous forest: uncertainty sources, stand structure effect, and future scenarios. Can. J. For. Res. 45, 1489–1497. https://doi.org/10.1139/cjfr-2015-0009.
Hyndman, R., Athanasopoulos, G., Bergmeir, C., Caceres, G., Chhay, L., O'Hara-Wild, M., Petropoulos, F., Razbash, S., Wang, E., Yasmeen, F., 2019. _forecast: forecasting functions for time series and linear models_.
Komatsu, H., Kume, T., Shinohara, Y., 2017. Optimal sap flux sensor allocation for stand transpiration estimates: a non-dimensional analysis. Ann. For. Sci. 74, 38. https://doi.org/10.1007/s13595-017-0638-x.
Kutscha, N.P., Sachs, I.B., 1968. Color tests for differentiating heartwood and sapwood in certain softwood tree species, U.S. Forestry Products Laboratory Report No. 2246. Madison, WI, USA. Madison, Wisconsin.
Lenth, R.V., 2018. emmeans: estimated marginal means, aka least-squares means. R package version 1.2.3. https://CRAN.R-project.org/package=emmeans.
Link, P., Simonin, K., Maness, H., Oshun, J., Dawson, T., Fung, I., 2014. Species differences in the seasonality of evergreen tree transpiration in a Mediterranean climate: analysis of multiyear, half-hourly sap flow observations. Water Resour. Res. 50, 1869–1894. https://doi.org/10.1002/2013WR014023.
Looker, N., Martin, J., Jencso, K., Hu, J., 2016. Contribution of sapwood traits to uncertainty in conifer sap flow as estimated with the heat-ratio method. Agric. For. Meteorol. 223, 60–71. https://doi.org/10.1016/J.AGRFORMET.2016.03.014.
López-Bernal, Á., Alcántara, E., Testi, L., Villalobos, F.J., 2010. Spatial sap flow and xylem anatomical characteristics in olive trees under different irrigation regimes. Tree Physiol. 30, 1536–1544. https://doi.org/10.1093/treephys/tpq095.
Lu, P., Urban, L., Zhao, P., 2004. Granier's thermal dissipation probre (TDP) method for measuring sap flow in trees : theory and practice. Acta Bot. Sin. 46, 631–646.
Marshall, D.C., 1958. Measurement of sap flow in conifers by heat transport. Plant Physiol. 33, 385–396. https://doi.org/10.1104/PP.33.6.385.
Oishi, A.C., Hawthorne, D.A., Oren, R., 2016. Baseliner: an open-source, interactive tool for processing sap flux data from thermal dissipation probes. SoftwareX 5, 139–143. https://doi.org/10.1016/J.SOFTX.2016.07.003.
Oishi, A.C., Oren, R., Stoy, P.C., 2008. Estimating components of forest evapotranspiration: a footprint approach for scaling sap flux measurements. Agric. For. Meteorol. 148, 1719–1732. https://doi.org/10.1016/J.AGRFORMET.2008.06.013.
Olbrich, B.W., 1991. The verification of the heat pulse velocity technique for estimating sap flow in *Eucalyptus grandis*. Can. J. For. Res. 21, 836–841. https://doi.org/10.1139/x91-117.
Peters, R.L., Fonti, P., Frank, D.C., Poyatos, R., Pappas, C., Kahmen, A., Carraro, V., Prendin, A.L., Schneider, L., Baltzer, J.L., Baron-Gafford, G.A., Dietrich, L., Heinrich, I., Minor, R.L., Sonnentag, O., Matheny, A.M., Wightman, M.G., Steppe, K., 2018. Quantification of uncertainties in conifer sap flow measured with the thermal dissipation method. New Phytol. 219, 1283–1299. https://doi.org/10.1111/nph.15241.
Pinheiro, J., Bates, D., DebRoy, S., Sarkar, D., R Core Team, 2018. _nlme: linear and nonlinear mixed effects models_. R Package Ver. 3, 1–137. URL. https://CRAN.R-project.org/package=nlme.
R Development Core Team, 2019. R: a language and environment for statistical computing.
Rabbel, I., Diekkrüger, B., Voigt, H., Neuwirth, B., Rabbel, I., Diekkrüger, B., Voigt, H., Neuwirth, B., 2016. Comparing ΔTmax determination approaches for Granier-based sapflow estimations. Sensors 16, 2042. https://doi.org/10.3390/s16122042.
Roberts, J., 1977. The use of tree-cutting techniques in the study of the water relations of mature *Pinus sylvestris* l. J. Exp. Bot 28, 751–767. https://doi.org/10.1093/jxb/28.3.751.
Sato, T., Oda, T., Igarashi, Y., Suzuki, M., Uchiyama, Y., 2012. Circumferential sap flow variation in the trunks of Japanese cedar and cypress trees growing on a steep slope. Hydrol. Res. Lett. 6, 104–108. https://doi.org/10.3178/hrl.6.104.
Schlesinger, W.H., Jasechko, S., 2014. Transpiration in the global water cycle. Agric. For. Meteorol. 189–190, 115–117. https://doi.org/10.1016/j.agrformet.2014.01.011.
Schneider, C.A., Rasband, W.S., Eliceiri, K.W., 2012. NIH image to ImageJ: 25 years of image analysis. Nat. Methods 9, 671–675. https://doi.org/10.1038/nmeth.2089.
Scholander, P.F., Bradstreet, E.D., Hemmingsen, E.A., Hammel, H.T., 1965. Sap pressure in vascular plants, negative hydrostatic pressure can be measured in plants. Science 148, 339–346. https://doi.org/10.1126/science.148.3668.33.
Shinohara, Y., Tsuruta, K., Ogura, A., Noto, F., Komatsu, H., Otsuki, K., Maruyama, T., 2013. Azimuthal and radial variations in sap flux density and effects on stand-scale transpiration estimates in a Japanese cedar forest. Tree Physiol 33, 550–558. https://doi.org/10.1093/treephys/tpt029.
Smith, R.E., 1992. The heat pulse velocity technique for determining water uptake of *Populus deltoides*. South African J. Bot. 58, 100–104. https://doi.org/10.1016/S0254-6299(16)30879-1.
Tseng, H., Chiu, C.-.W., Laplace, S., Kume, T., 2017. Can we assume insignificant temporal changes in spatial variations of sap flux for year-round individual tree transpiration estimates? A case study on *Cryptomeria japonica* in central Taiwan. Trees 31, 1239–1251. https://doi.org/10.1007/s00468-017-1542-6.
Van de Wal, B.A.E., Guyot, A., Lovelock, C.E., Lockington, D.A., Steppe, K., 2015. Influence of temporospatial variation in sap flux density on estimates of whole-tree water use in *Avicennia marina*. Trees 29, 215–222. https://doi.org/10.1007/s00468-014-1105-z.
Vandegehuchte, M.W., Burgess, S.S.O., Downey, A., Steppe, K., 2015. Influence of stem temperature changes on heat pulse sap flux density measurements. Tree Physiol. 35, 346–353. https://doi.org/10.1093/treephys/tpu068.
Vergeynst, L.L., Vandegehuchte, M.W., McGuire, M.A., Teskey, R.O., Steppe, K., 2014. Changes in stem water content influence sap flux density measurements with thermal dissipation probes. Trees 28, 949–955. https://doi.org/10.1007/s00468-014-0989-y.
Vertessy, R.A., Hatton, T.J., Reece, P., O'Sullivan, S.K., Benyon, R.G., 1997. Estimating stand water use of large mountain ash trees and validation of the sap flow measurement technique. Tree Physiol. 17, 747–756. https://doi.org/10.1093/treephys/17.12.747.
Ward, E.J., 2016. Measuring water fluxes in forests: the need for integrative platforms of analysis. Tree Physiol. 36, 929–931. https://doi.org/10.1093/treephys/tpw065.
Wullschleger, S.D., King, A.W., 2000. Radial variation in sap velocity as a function of stem diameter and sapwood thickness in yellow-poplar trees. Tree Physiol. 20, 511–518. https://doi.org/10.1093/treephys/20.8.511.
Zhang, Y., Peña-Arancibia, J.L., McVicar, T.R., Chiew, F.H.S., Vaze, J., Liu, C., Lu, X., Zheng, H., Wang, Y., Liu, Y.Y., Miralles, D.G., Pan, M., 2016. Multi-decadal trends in global terrestrial evapotranspiration and its components. Sci. Rep. 6, 19124. https://doi.org/10.1038/srep19124.
Zhang, Z., Zhao, Ping, Zhao, X., Zhou, J., Zhao, Peiqiang, Zeng, X., Hu, Y., Ouyang, L., 2018. The tree height-related spatial variances of tree sap flux density and its scale-up to stand transpiration in a subtropical evergreen broadleaf forest. Ecohydrology 11, e1979. https://doi.org/10.1002/eco.1979.